

Concept Study of High Frequency Telescope for LiteBIRD

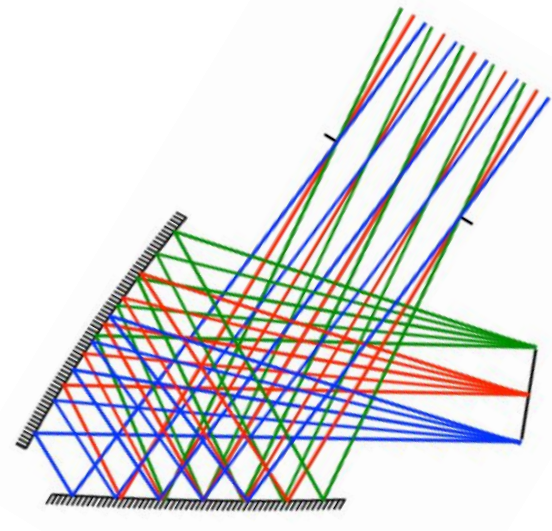
Takashi Hasebe and LiteBIRD Collaboration

National Astronomical Observatory of Japan

Introduction

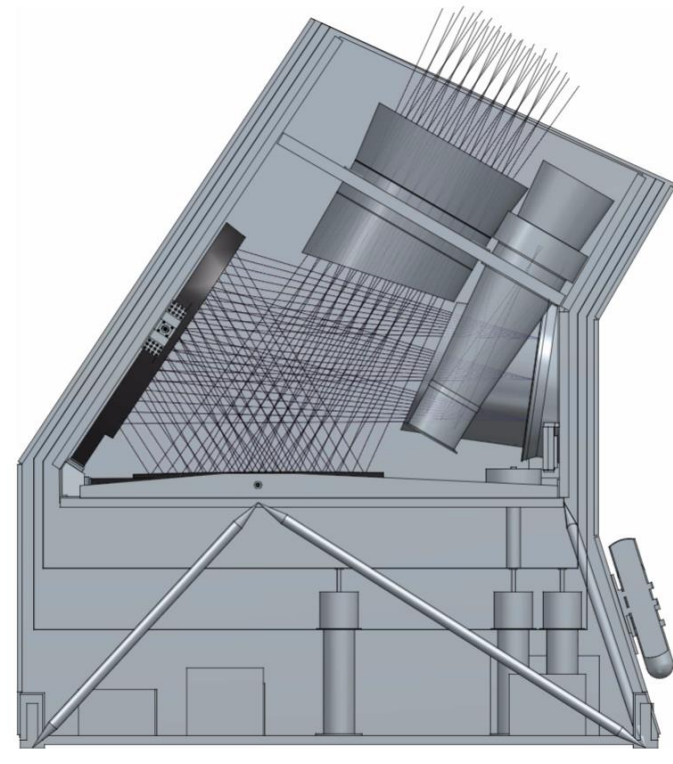
Low Frequency Telescope (LFT)

40 – 235 GHz

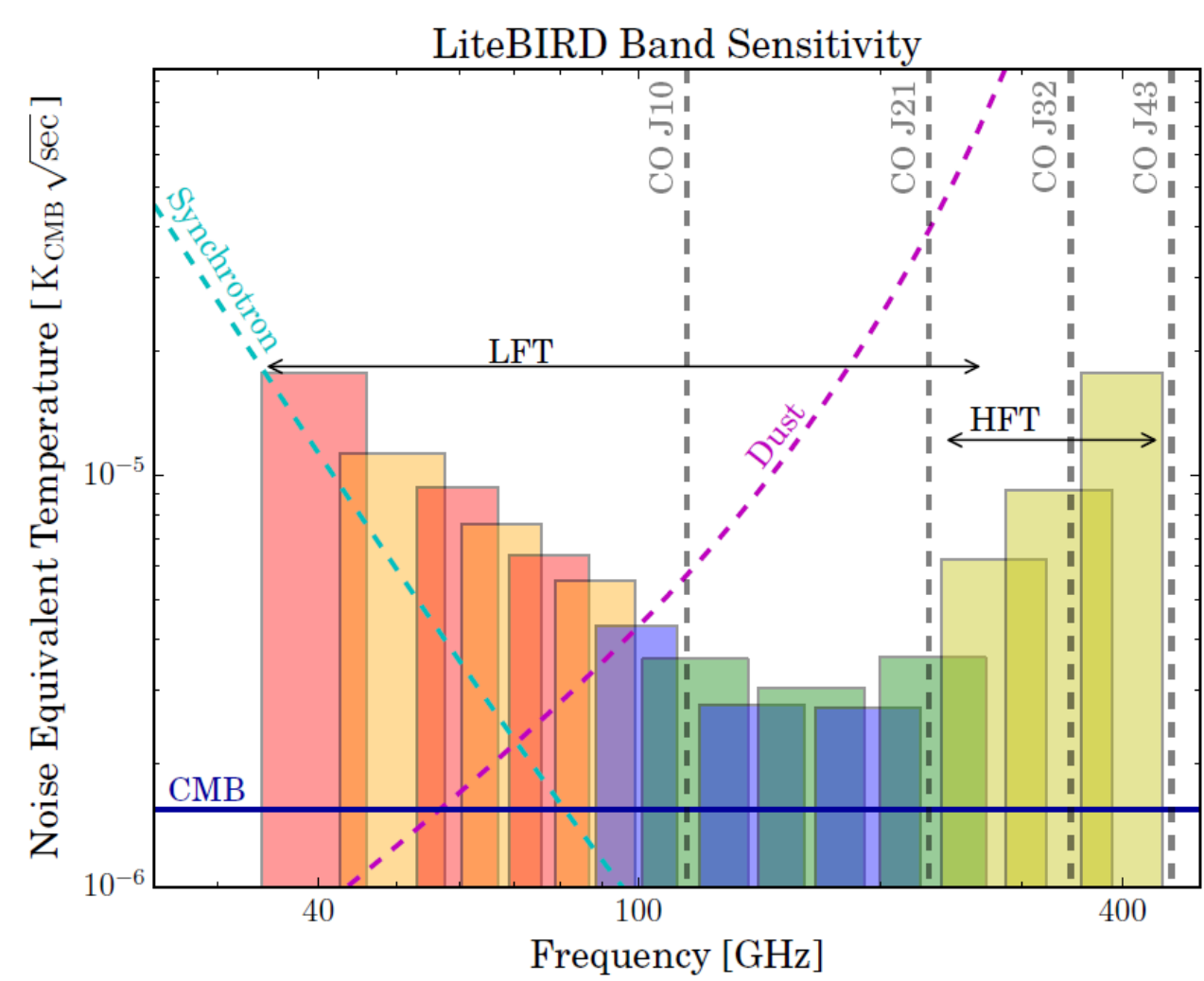


High Frequency Telescope (HFT)

280 – 402 GHz

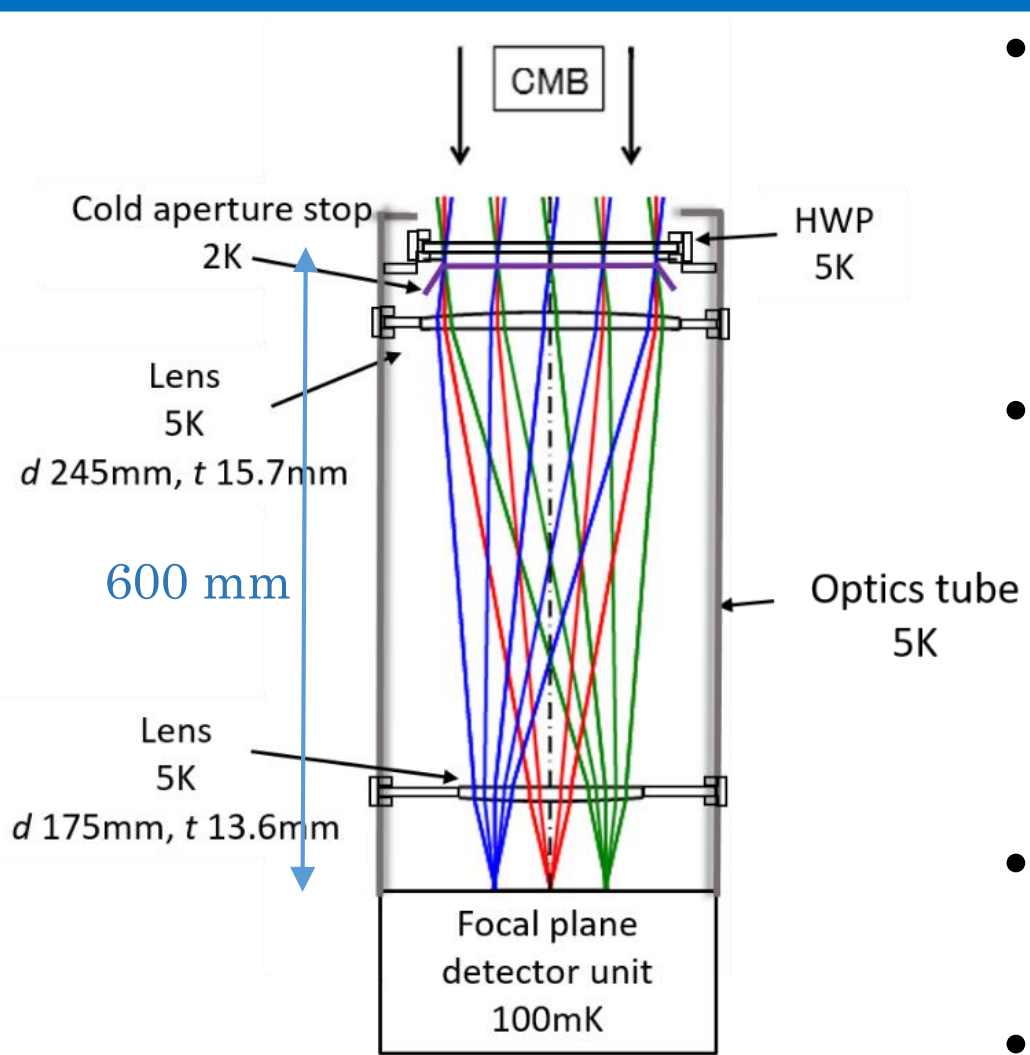


- LiteBIRD is a satellite mission to be launched by JAXA for verification of inflation at the beginning of the universe via the B-mode polarization of the CMB.
- For the purpose of the broadband and wide field observations of the all sky, LiteBIRD receives frequency bands of 40 – 402 GHz with two telescopes, LFT and HFT [1].



- The precise measurement of the B-mode signal requires the removal of contaminating polarized emissions, mainly from synchrotron and thermal dust.
- In order to separate these foreground emissions, the observations of the broad frequency spectrum of them are necessary.

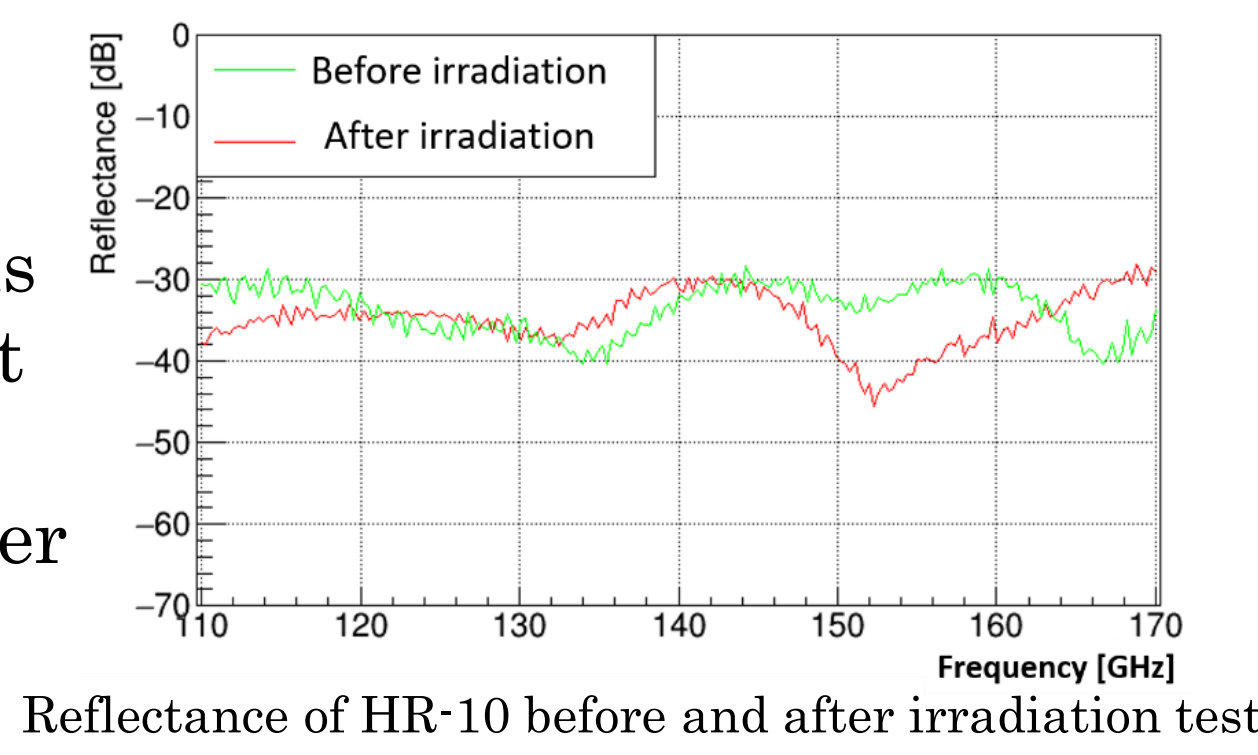
HFT Baseline Design



① Baseline design

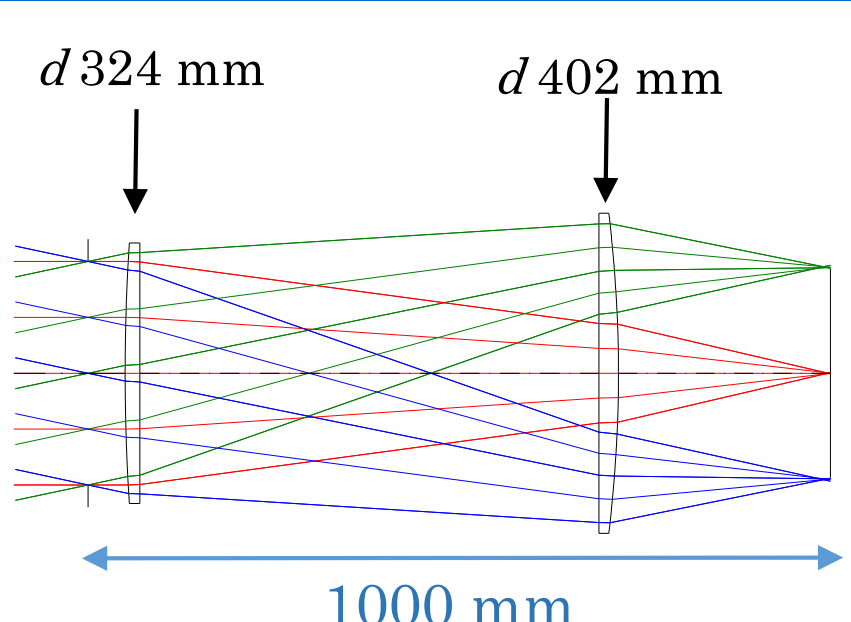
- The optical design of the HFT basically follows typical refractive telescopes for CMB observations[2,3,4]. The HFT consists of a continuous - rotating HWP, two silicon lenses and focal plane detectors.
- In order to suppress thermal emissions from the optical elements, all components are cooled down to less than 5 K. Superconducting detectors at the focal plane operate at 100 mK for extremely low-noise detection.
- 2 K aperture stop suppress thermal loading of spillover at the entrance pupil.
- Heat loads to 5 K stage are mainly come from support structure and detector readout. Their heat dissipations are estimated to be 0.7 mW and 0.2 mW, respectively.

- The optical components are covered by HR-10 pasted to the inner wall of the optics tube. The reflectance of HR-10 at millimeter wavelength is less than -30 dB. The radiation degradation of it was measured for space use. No significant degradation was found from 110 to 170 GHz after exposed to 10 krad radiation(equivalent to 5 years exposure at L2 orbit).

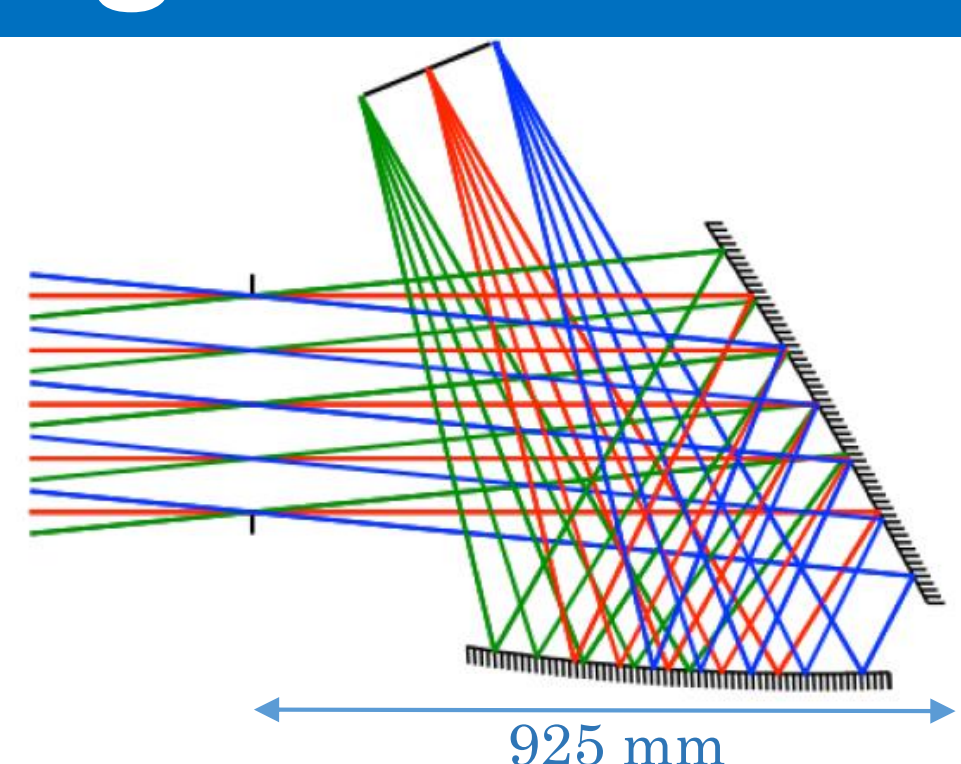


Reflectance of HR-10 before and after irradiation test

Large HFT Designs

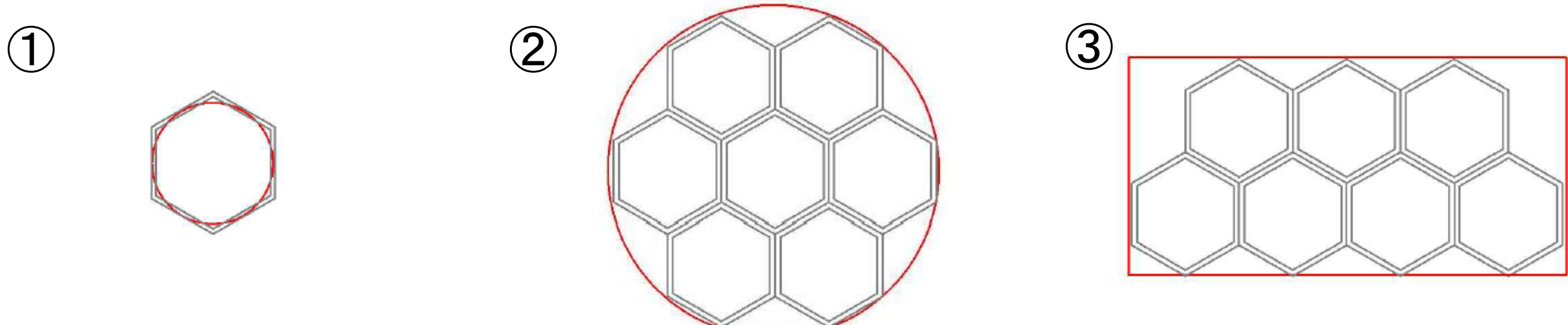


② Large refractive design



③ Reflective design

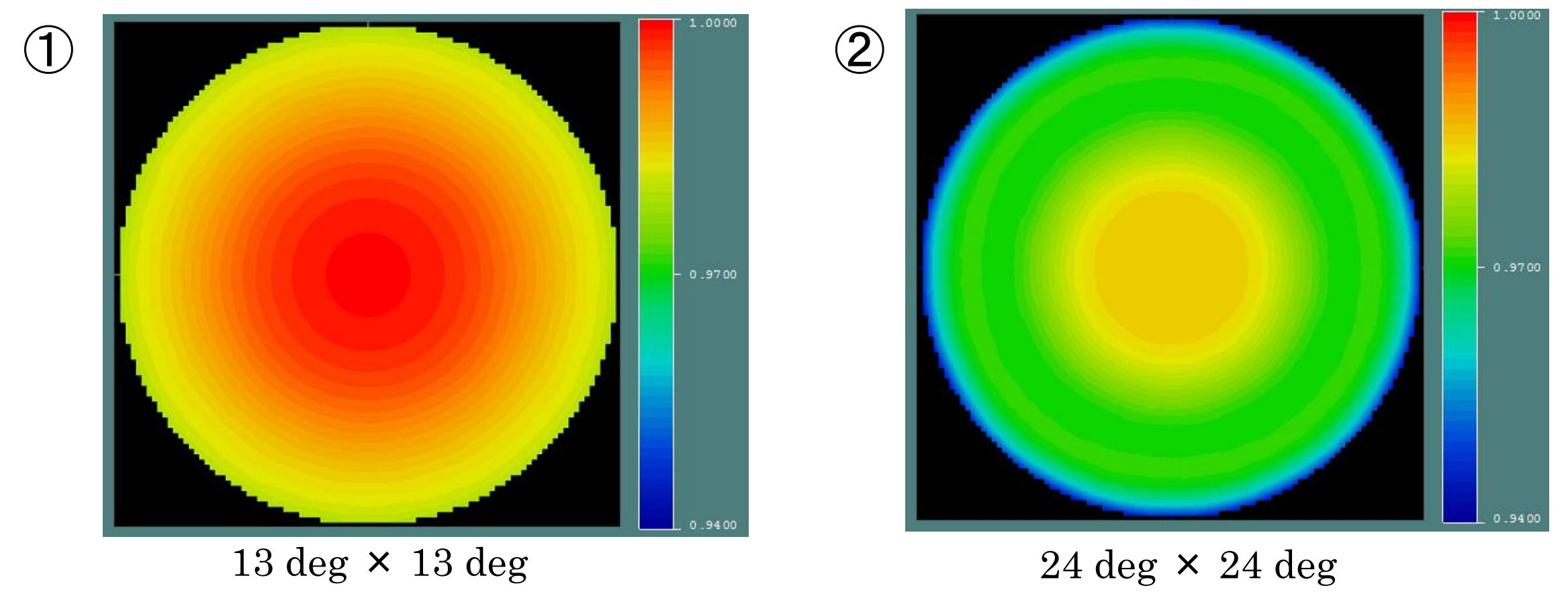
- The bigger HFT which has larger aperture and wider field-of-view has been studied to put more detectors at the focal plane.
- The larger focal plane area and broader frequency range improve the sensitivity of the CMB and foreground channels.



Schematic views of the focal plane area and detector array of each design.

Acknowledgement

This work is supported by MEXT KAKENHI Grant Number 17H01115 and 15H05891. The irradiation test was supported by Research Project with Heavy Ions at NIRS-HIMAC.



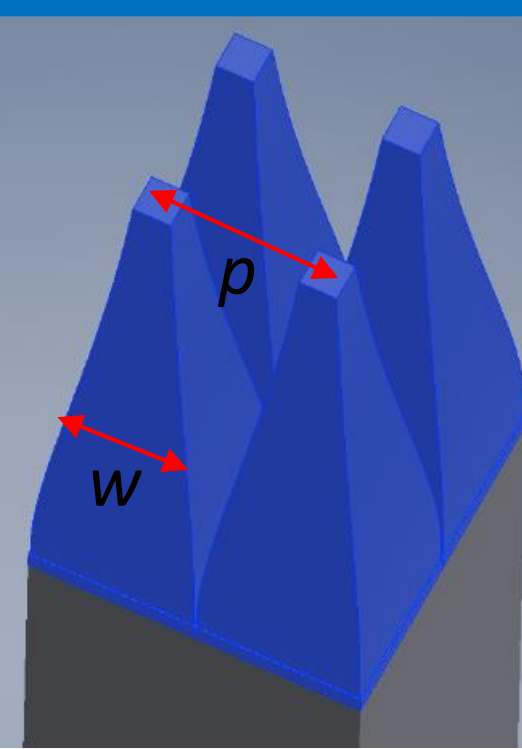
Strehl ratios of model ① and ② achieve more than 0.975 and 0.94 at 450 GHz, respectively.

Model	Frequency (edge to edge) [GHz]	Aperture Diameter [mm]	F#	Field of View [deg ²]	Focal Plane Area [mm ²]	Mass [kg]	Heat load to 5K stage [mW]
①	248 - 448	200	2.2	Φ13	Φ102	21	0.9 ^{*1}
②	101 - 448	300	2.2	Φ24	Φ280	49	3.3 ^{*1}
③	101 - 448	300	3.5	20 × 10	370 × 184	56	2.8 ^{*2}

1. Assume 384 bolometers and 6 SQUIDS. 2. Assume 4000 bolometers and 60 SQUIDS. 3. Assume 2000 bolometers and 30 SQUIDS

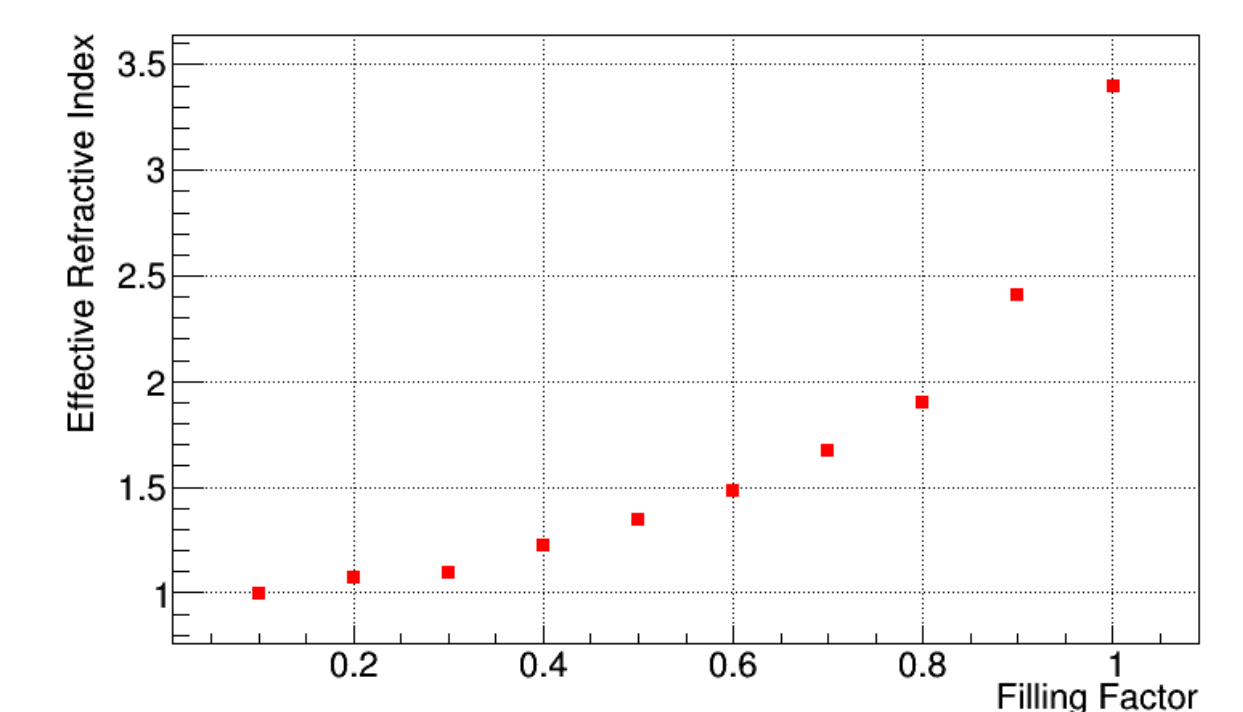
- The key component of the broadband HFT is the AR coating development of the silicon lenses from 100GHz to 450GHz.
- The reflectors option can avoid this technical challenge, however the size of the 5 K cryogenics part and the entire satellite system become larger.

AR Coating for Silicon Lens

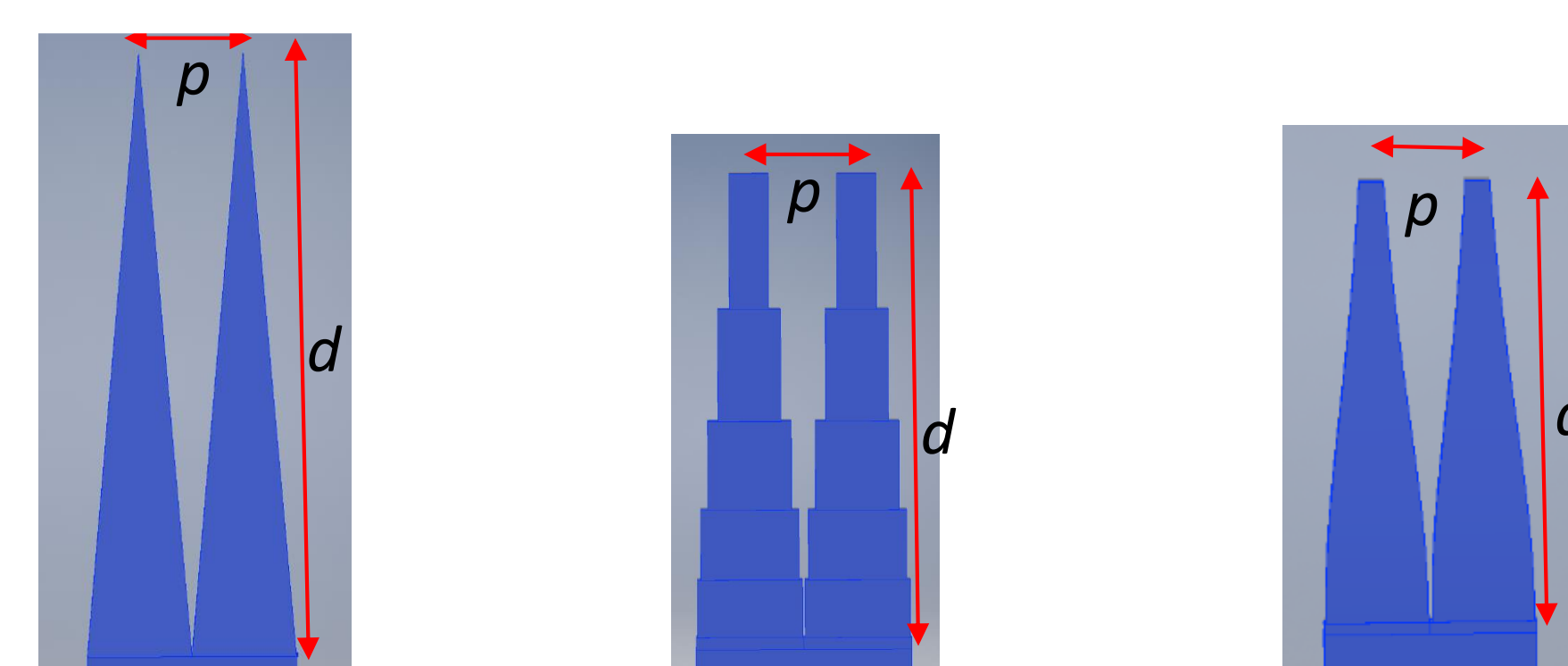


- AR coating on silicon lens for the HFT requires less than 5 % reflection to achieve better sensitivity than that of the HFT with reflectors option.
- AR surface with subwavelength structure (SWS) on silicon has been reported for millimeter wave applications [5,6].
- The SWS AR coated silicon which covers the frequency range of the HFT baseline design, 248 - 448 GHz, was demonstrated by [7].
- Three types of SWS [8,9] which covers the frequency range of the large HFT design, 101- 448 GHz, are simulated by HFSS.
- The pitch of the periodical structure is determined by $p < \lambda_{\min} / n$, where λ_{\min} is the minimum wavelength of the incident wave and n is the refractive index of the material.

- The effective refractive index of the subwavelength structure is defined by the filling factor of the material as $F = w / p$.
- The right figure shows relation between the filling factor and the effective refractive index at $p = 180 \mu\text{m}$. Data points are given by comparison of reflections of the dielectric membrane and the subwavelength structures simulated by HFSS.



The relation between filling factor and effective refractive index simulated by HFSS.

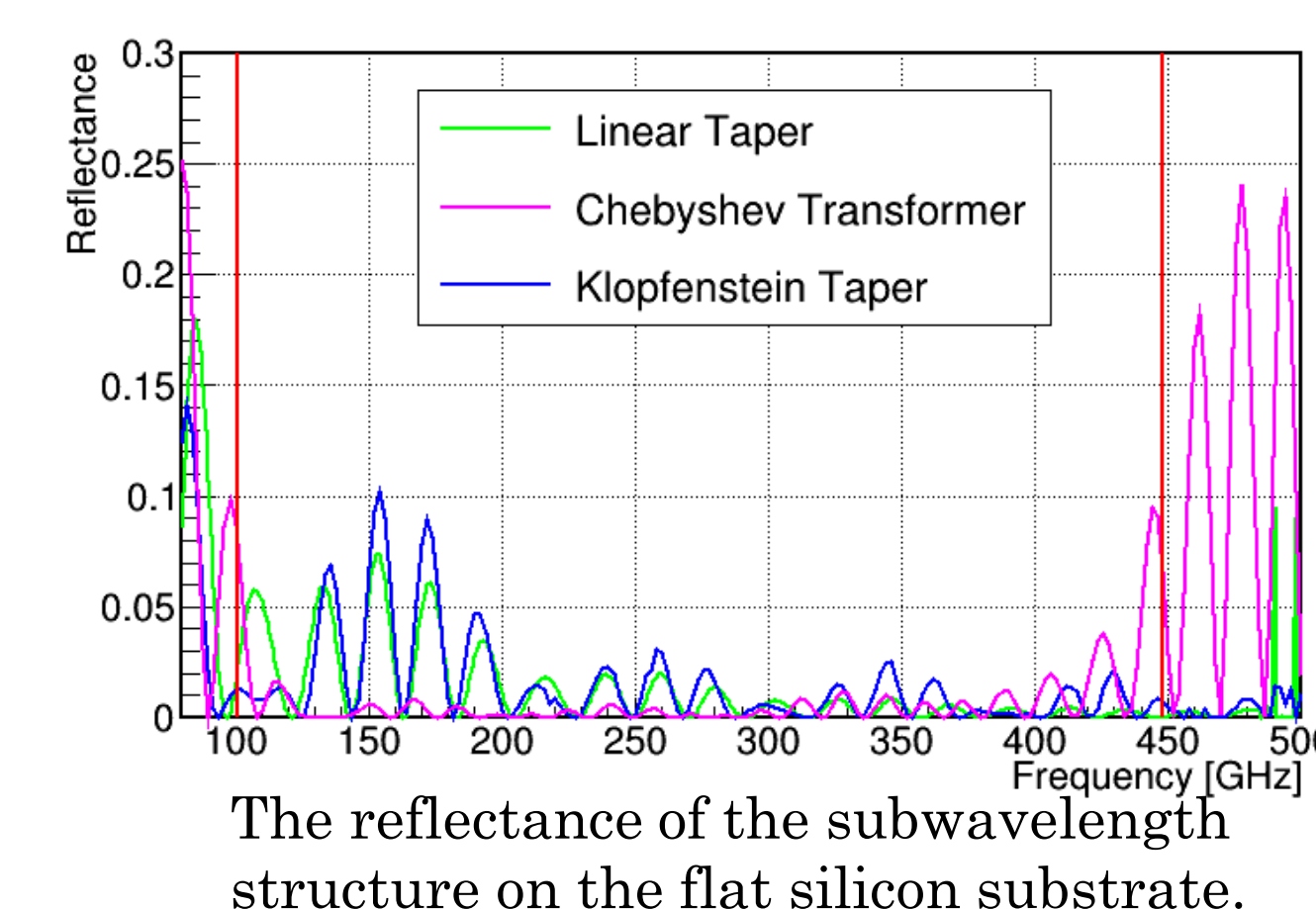


Model	p [μm]	d [μm]	r
①	180	1000	0.1
②	180	776	0.1
③	180	752	0.08

r : designed value of the maximum reflection coefficient

① Linear Taper ② Chebyshev Transformer ③ Klopfenstein Taper

- Three types of solutions to achieve AR requirement for HFT are demonstrated.
- Each structure is modeled on both sides of the 2.0mm flat silicon substrate.



The reflectance of the subwavelength structure on the flat silicon substrate.

- The large ripples are seen around 150 GHz at continuous structures.
- The possible reason is mismatch of the refractive index near the silicon substrate due to a large uncertainty of transformation of refractive index into filling factor.
- The discrete structure of the 5 layers Chebyshev transformer shows better performance and its aspect ratio is 4.3.

Summary

- The optical designs of the HFT including options which has larger focal plane and broader frequency range has been studied.
- The antireflection coating for silicon lenses with subwavelength structure for the large HFT design was simulated. The reflectance achieves less than 5 % from 100 to 450 GHz on band average.

References

1. Sugai, H et al., "Optical designing of LiteBIRD", *Proc. SPIE* 9904 (2016).
2. Rahlin, A.S et al., "Pre-flight integration and characterization of the SPIDER balloon-borne telescope", *Proc. of SPIE*, Vol. 9153, 915313-1.
3. Ade, P.A.R et al., "BICEP2/KECK ARRAY. IV. Optical Characterization and Performance of the BICEP2 and KECK Array Experiments", *Astro. Phys. J.*, 806 : 206 (2015).
4. Bock, J et al., "The Experimental Probe of Inflationary Cosmology (EPIC): A Mission Concept Study for NASA's Einstein Inflation Probe", *arXiv* 0805.4207 [astro-ph]
5. Datta, R et al., "Large-aperture wide-bandwidth antireflection-coated silicon lenses for millimeter wavelength", *Applied Optics*, Vol.52, No.36, 8747 (2013).
6. Nitta, T et al., "Broadband Pillar-Type Antireflective Subwavelength Structures for Silicon and Alumina", *IEEE Transactions on Terahertz and Technology*, Vol.7, No.3 (2017).
7. Young, K et al., "Broadband Millimeter-Wave Anti-Reflection Coatings on Silicon Using Pyramidal Sub-Wavelength Structures", *J. Applied Phys.* 121, 213103 (2017).
8. Matsumura, T et al., "Millimeter-wave broadband antireflection coatings using laser ablation of subwavelength structures", *Applied Optics*, Vol.55, No.13, 3502 (2016).
9. Grann, Eric.B. and Moharam, M.G. "Comparison between continuous and discrete subwavelength grating structures for antireflection surfaces", *J. Opt. Soc. Am. A*, Vol.13, No.5 (1996).